

# Detection of the ISW effect and corresponding dark energy constraints

(astro-ph/0602398)

Jason McEwen<sup>1</sup>

with P. Vielva<sup>2,3</sup>, M. P. Hobson<sup>1</sup>,  
E. Martínez-González<sup>2</sup> and A. N. Lasenby<sup>1</sup>

<sup>1</sup>Cavendish Laboratory, University of Cambridge

<sup>2</sup>Instituto de Física de Cantabria, Universidad de Cantabria

<sup>3</sup>Laboratoire APC, Collège de France

Rencontres de Moriond :: 23 March 2006

# Outline

- 1 Integrated Sachs-Wolfe (ISW) effect
  - Physical origin
  - Detecting the effect
- 2 The continuous spherical wavelet transform (CSWT)
  - Dilations and mother wavelets on the sphere
  - Transform
- 3 Cross-correlation in wavelet space
  - Wavelet covariance estimator
  - Comparison of wavelets
- 4 Analysis procedure
- 5 Results
  - Detections
  - Dark energy constraints
- 6 Summary

# Outline

- 1 Integrated Sachs-Wolfe (ISW) effect
  - Physical origin
  - Detecting the effect
- 2 The continuous spherical wavelet transform (CSWT)
  - Dilations and mother wavelets on the sphere
  - Transform
- 3 Cross-correlation in wavelet space
  - Wavelet covariance estimator
  - Comparison of wavelets
- 4 Analysis procedure
- 5 Results
  - Detections
  - Dark energy constraints
- 6 Summary

# ISW effect

## Physical origin

- Photons blue (red) shifted when fall into (out of) potential wells
- Evolution of potential during photon propagation  
→ net change in photon energy
- Large scale phenomenon  
(cosmic variance limited → require full-sky maps)
- Only present in non-flat universes or flat universes with dark energy

Temperature perturbation

$$\frac{\delta T}{T} = 2 \int \frac{\dot{\Phi}}{c^2} \frac{d\ell}{c}$$

where  $d\ell$  is the element of proper distance. In Einstein de-Sitter universe (no  $\Lambda$ ),  $\Phi_k \sim \delta_k/a$  and linear growth law for  $\Omega = 1$  is  $\delta_k \sim a$ . Thus  $\dot{\Phi} \neq 0$  only when  $\Omega$  diverges significantly from unity.

# ISW effect

## Physical origin

- Photons blue (red) shifted when fall into (out of) potential wells
- Evolution of potential during photon propagation  
→ net change in photon energy
- Large scale phenomenon  
(cosmic variance limited → require full-sky maps)
- Only present in non-flat universes or flat universes with dark energy

Temperature perturbation

$$\frac{\delta T}{T} = 2 \int \frac{\dot{\Phi}}{c^2} \frac{d\ell}{c}$$

where  $d\ell$  is the element of proper distance. In Einstein de-Sitter universe (no  $\Lambda$ ),  $\Phi_k \sim \delta_k/a$  and linear growth law for  $\Omega = 1$  is  $\delta_k \sim a$ . Thus  $\dot{\Phi} \neq 0$  only when  $\Omega$  diverges significantly from unity.

# ISW effect

## Physical origin

- Photons blue (red) shifted when fall into (out of) potential wells
- Evolution of potential during photon propagation  
→ net change in photon energy
- Large scale phenomenon  
(cosmic variance limited → require full-sky maps)
- Only present in non-flat universes or flat universes with dark energy

Temperature perturbation

$$\frac{\delta T}{T} = 2 \int \frac{\dot{\Phi}}{c^2} \frac{d\ell}{c}$$

where  $d\ell$  is the element of proper distance. In Einstein de-Sitter universe (no  $\Lambda$ ),  $\Phi_k \sim \delta_k/a$  and linear growth law for  $\Omega = 1$  is  $\delta_k \sim a$ . Thus  $\dot{\Phi} \neq 0$  only when  $\Omega$  diverges significantly from unity.

# ISW effect

## Physical origin

- Photons blue (red) shifted when fall into (out of) potential wells
- Evolution of potential during photon propagation  
→ net change in photon energy
- Large scale phenomenon  
(cosmic variance limited → require full-sky maps)
- Only present in non-flat universes or flat universes with dark energy

Temperature perturbation

$$\frac{\delta T}{T} = 2 \int \frac{\dot{\Phi}}{c^2} \frac{d\ell}{c}$$

where  $d\ell$  is the element of proper distance. In Einstein de-Sitter universe (no  $\Lambda$ ),  $\Phi_k \sim \delta_k/a$  and linear growth law for  $\Omega = 1$  is  $\delta_k \sim a$ . Thus  $\dot{\Phi} \neq 0$  only when  $\Omega$  diverges significantly from unity.

# Detecting the ISW effect

## Cross-correlating the CMB with LSS

- Cannot directly separate the ISW signal from CMB anisotropies
- Detected by cross-correlating CMB anisotropies with tracers of large scale structure (Crittenden & Turok 1996)
- Detections used to place constraints on dark energy
- Previous works
  - Real space angular correlation function (e.g. Boughn & Crittenden 2002)
  - Harmonic space cross-angular power spectrum (e.g. Afshordi et al. 2004)
  - Azimuthally symmetric wavelet covariance (Vielva et al. 2006)
- We extend spherical wavelet approach to directional wavelets (no reason to expect azimuthally symmetric structures)



# Detecting the ISW effect

## Cross-correlating the CMB with LSS

- Cannot directly separate the ISW signal from CMB anisotropies
- Detected by cross-correlating CMB anisotropies with tracers of large scale structure (Crittenden & Turok 1996)
- Detections used to place constraints on dark energy
- Previous works
  - Real space angular correlation function (e.g. Boughn & Crittenden 2002)
  - Harmonic space cross-angular power spectrum (e.g. Afshordi et al. 2004)
  - Azimuthally symmetric wavelet covariance (Vielva et al. 2006)
- We extend spherical wavelet approach to directional wavelets (no reason to expect azimuthally symmetric structures)

# Detecting the ISW effect

## Cross-correlating the CMB with LSS

- Cannot directly separate the ISW signal from CMB anisotropies
- Detected by cross-correlating CMB anisotropies with tracers of large scale structure (Crittenden & Turok 1996)
- Detections used to place constraints on dark energy
- Previous works
  - Real space angular correlation function (e.g. Boughn & Crittenden 2002)
  - Harmonic space cross-angular power spectrum (e.g. Afshordi et al. 2004)
  - Azimuthally symmetric wavelet covariance (Vielva et al. 2006)
- We extend spherical wavelet approach to directional wavelets (no reason to expect azimuthally symmetric structures)

# Detecting the ISW effect

## Cross-correlating the CMB with LSS

- Cannot directly separate the ISW signal from CMB anisotropies
- Detected by cross-correlating CMB anisotropies with tracers of large scale structure (Crittenden & Turok 1996)
- Detections used to place constraints on dark energy
- Previous works
  - Real space angular correlation function (e.g. Boughn & Crittenden 2002)
  - Harmonic space cross-angular power spectrum (e.g. Afshordi et al. 2004)
  - Azimuthally symmetric wavelet covariance (Vielva et al. 2006)
- We extend spherical wavelet approach to directional wavelets (no reason to expect azimuthally symmetric structures)

# Detecting the ISW effect

## Cross-correlating the CMB with LSS

- Cannot directly separate the ISW signal from CMB anisotropies
- Detected by cross-correlating CMB anisotropies with tracers of large scale structure (Crittenden & Turok 1996)
- Detections used to place constraints on dark energy
- Previous works
  - Real space angular correlation function (e.g. Boughn & Crittenden 2002)
  - Harmonic space cross-angular power spectrum (e.g. Afshordi et al. 2004)
  - Azimuthally symmetric wavelet covariance (Vielva et al. 2006)
- We extend spherical wavelet approach to directional wavelets (no reason to expect azimuthally symmetric structures)

# Outline

- 1 Integrated Sachs-Wolfe (ISW) effect
  - Physical origin
  - Detecting the effect
- 2 **The continuous spherical wavelet transform (CSWT)**
  - Dilations and mother wavelets on the sphere
  - Transform
- 3 Cross-correlation in wavelet space
  - Wavelet covariance estimator
  - Comparison of wavelets
- 4 Analysis procedure
- 5 Results
  - Detections
  - Dark energy constraints
- 6 Summary

# Spherical wavelet transform

## Anisotropic dilation on the sphere

- Spherical wavelet transform (Antoine and Vandergheynst 1998; Wiaux et al. 2005)
- Stereographic projection  $\Pi$
- Anisotropic dilation on the sphere

$$\mathcal{D}(a, b) = \Pi^{-1} d(a, b) \Pi$$

$$[\mathcal{D}(a, b)s](\omega) = [\lambda(a, b, \theta, \phi)]^{1/2} s(\omega_{1/a, 1/b})$$

where

$$\omega_{a,b} = (\theta_{a,b}, \phi_{a,b}),$$

$$\tan(\theta_{a,b}/2) = \tan(\theta/2) \sqrt{a^2 \cos^2 \phi + b^2 \sin^2 \phi}$$

$$\tan(\phi_{a,b}) = \frac{b}{a} \tan(\phi)$$

# Spherical wavelet transform

## Anisotropic dilation on the sphere

- Spherical wavelet transform (Antoine and Vandergheynst 1998; Wiaux et al. 2005)
- Stereographic projection  $\Pi$
- Anisotropic dilation on the sphere

$$D(a, b) = \Pi^{-1} d(a, b) \Pi$$

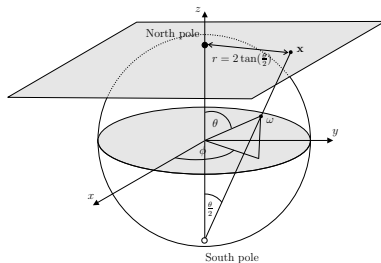
$$[D(a, b)s](\omega) = [\lambda(a, b, \theta, \phi)]^{1/2} s(\omega_{1/a, 1/b})$$

where

$$\omega_{a,b} = (\theta_{a,b}, \phi_{a,b}),$$

$$\tan(\theta_{a,b}/2) = \tan(\theta/2) \sqrt{a^2 \cos^2 \phi + b^2 \sin^2 \phi}$$

$$\tan(\phi_{a,b}) = \frac{b}{a} \tan(\phi)$$



# Spherical wavelet transform

## Anisotropic dilation on the sphere

- Spherical wavelet transform (Antoine and Vandergheynst 1998; Wiaux et al. 2005)
- Stereographic projection  $\Pi$
- Anisotropic dilation on the sphere

$$\mathcal{D}(a, b) = \Pi^{-1} d(a, b) \Pi$$

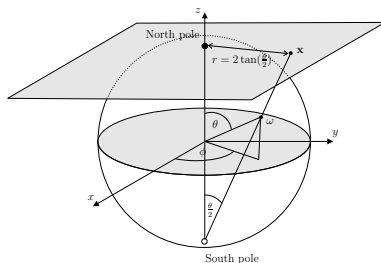
$$[\mathcal{D}(a, b)s](\omega) = [\lambda(a, b, \theta, \phi)]^{1/2} s(\omega_{1/a, 1/b})$$

where

$$\omega_{a,b} = (\theta_{a,b}, \phi_{a,b}),$$

$$\tan(\theta_{a,b}/2) = \tan(\theta/2) \sqrt{a^2 \cos^2 \phi + b^2 \sin^2 \phi}$$

$$\tan(\phi_{a,b}) = \frac{b}{a} \tan(\phi)$$





# Spherical wavelet transform

## Mother wavelets on the sphere

- Stereographic projection of admissible Euclidean mother wavelets

$$\psi(\omega) = [\Pi^{-1}\psi_{\mathbb{R}^2}](\omega)$$

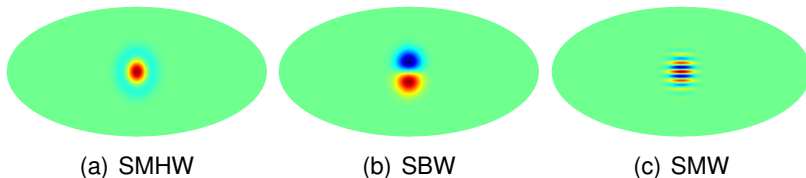


Figure: Spherical wavelets at scale  $a = b = 0.2$ .

# Spherical wavelet transform

- Motion on the sphere ( $\equiv$  rotation)

$$[R(\rho)s](\omega) = s(\rho^{-1}\omega), \quad \rho \in \text{SO}(3)$$

- Multi-resolution basis on the sphere

$$\{\psi_{a,b,\rho} \equiv R(\rho)\mathcal{D}(a,b)\psi; \rho \in \text{SO}(3); a, b \in \mathbb{R}_*^+\}$$

- Spherical wavelet transform

$$W_\psi(a, b, \rho) \equiv \int_{S^2} d\Omega(\omega) \psi_{a,b,\rho}^*(\omega) s(\omega)$$

- Fast algorithm (McEwen et al. 2005; Wandelt & Gorski 2001)

# Spherical wavelet transform

- Motion on the sphere ( $\equiv$  rotation)

$$[R(\rho)s](\omega) = s(\rho^{-1}\omega), \quad \rho \in \text{SO}(3)$$

- Multi-resolution basis on the sphere

$$\{\psi_{a,b,\rho} \equiv R(\rho)\mathcal{D}(a,b)\psi; \rho \in \text{SO}(3); a, b \in \mathbb{R}_*^+\}$$

- Spherical wavelet transform

$$W_\psi(a, b, \rho) \equiv \int_{S^2} d\Omega(\omega) \psi_{a,b,\rho}^*(\omega) s(\omega)$$

- Fast algorithm (McEwen et al. 2005; Wandelt & Gorski 2001)

# Spherical wavelet transform

- Motion on the sphere ( $\equiv$  rotation)

$$[R(\rho)s](\omega) = s(\rho^{-1}\omega), \quad \rho \in \text{SO}(3)$$

- Multi-resolution basis on the sphere

$$\{\psi_{a,b,\rho} \equiv R(\rho)\mathcal{D}(a,b)\psi; \rho \in \text{SO}(3); a, b \in \mathbb{R}_*^+\}$$

- Spherical wavelet transform

$$W_\psi(a, b, \rho) \equiv \int_{S^2} d\Omega(\omega) \psi_{a,b,\rho}^*(\omega) s(\omega)$$

- Fast algorithm (McEwen et al. 2005; Wandelt & Gorski 2001)

# Spherical wavelet transform

- Motion on the sphere ( $\equiv$  rotation)

$$[R(\rho)s](\omega) = s(\rho^{-1}\omega), \quad \rho \in \text{SO}(3)$$

- Multi-resolution basis on the sphere

$$\{\psi_{a,b,\rho} \equiv R(\rho)\mathcal{D}(a,b)\psi; \rho \in \text{SO}(3); a, b \in \mathbb{R}_*^+\}$$

- Spherical wavelet transform

$$W_\psi(a, b, \rho) \equiv \int_{S^2} d\Omega(\omega) \psi_{a,b,\rho}^*(\omega) s(\omega)$$

- Fast algorithm (McEwen et al. 2005; Wandelt & Gorski 2001)

# Outline

- 1 Integrated Sachs-Wolfe (ISW) effect
  - Physical origin
  - Detecting the effect
- 2 The continuous spherical wavelet transform (CSWT)
  - Dilations and mother wavelets on the sphere
  - Transform
- 3 Cross-correlation in wavelet space**
  - Wavelet covariance estimator**
  - Comparison of wavelets**
- 4 Analysis procedure
- 5 Results
  - Detections
  - Dark energy constraints
- 6 Summary

# Wavelet covariance estimator

- Suitability of wavelets for detecting cross-correlations
- Wavelet covariance

$$\hat{X}_{\psi}^{\text{NT}}(a, b, \gamma) = \frac{1}{N_{\alpha\beta}} \sum_{\alpha, \beta} \nu_{\alpha\beta} W_{\psi}^{\text{N}}(a, b, \alpha, \beta, \gamma) W_{\psi}^{\text{T}}(a, b, \alpha, \beta, \gamma)$$

- Average over orientations

$$\hat{X}_{\psi}^{\text{NT}}(a, b) = \frac{1}{N_{\gamma}} \sum_{\gamma} \hat{X}_{\psi}^{\text{NT}}(a, b, \gamma)$$

- Theoretical wavelet covariance

$$X_{\psi}^{\text{NT}}(a, b, \gamma) = \sum_{\ell=0}^{\infty} p_{\ell}^2 b_{\ell}^{\text{N}} b_{\ell}^{\text{T}} C_{\ell}^{\text{NT}} \sum_{m=-\ell}^{\ell} |(\psi_{a,b})_{\ell m}|^2$$

# Wavelet covariance estimator

- Suitability of wavelets for detecting cross-correlations
- Wavelet covariance

$$\hat{X}_{\psi}^{\text{NT}}(\mathbf{a}, \mathbf{b}, \gamma) = \frac{1}{N_{\alpha\beta}} \sum_{\alpha, \beta} \nu_{\alpha\beta} W_{\psi}^{\text{N}}(\mathbf{a}, \mathbf{b}, \alpha, \beta, \gamma) W_{\psi}^{\text{T}}(\mathbf{a}, \mathbf{b}, \alpha, \beta, \gamma)$$

- Average over orientations

$$\hat{X}_{\psi}^{\text{NT}}(\mathbf{a}, \mathbf{b}) = \frac{1}{N_{\gamma}} \sum_{\gamma} \hat{X}_{\psi}^{\text{NT}}(\mathbf{a}, \mathbf{b}, \gamma)$$

- Theoretical wavelet covariance

$$X_{\psi}^{\text{NT}}(\mathbf{a}, \mathbf{b}, \gamma) = \sum_{\ell=0}^{\infty} p_{\ell}^2 b_{\ell}^{\text{N}} b_{\ell}^{\text{T}} C_{\ell}^{\text{NT}} \sum_{m=-\ell}^{\ell} |(\psi_{\mathbf{a}, \mathbf{b}})_{\ell m}|^2$$



# Wavelet covariance estimator

- Suitability of wavelets for detecting cross-correlations
- Wavelet covariance

$$\hat{X}_{\psi}^{\text{NT}}(\mathbf{a}, \mathbf{b}, \gamma) = \frac{1}{N_{\alpha\beta}} \sum_{\alpha, \beta} \nu_{\alpha\beta} W_{\psi}^{\text{N}}(\mathbf{a}, \mathbf{b}, \alpha, \beta, \gamma) W_{\psi}^{\text{T}}(\mathbf{a}, \mathbf{b}, \alpha, \beta, \gamma)$$

- Average over orientations

$$\hat{X}_{\psi}^{\text{NT}}(\mathbf{a}, \mathbf{b}) = \frac{1}{N_{\gamma}} \sum_{\gamma} \hat{X}_{\psi}^{\text{NT}}(\mathbf{a}, \mathbf{b}, \gamma)$$

- Theoretical wavelet covariance

$$X_{\psi}^{\text{NT}}(\mathbf{a}, \mathbf{b}, \gamma) = \sum_{\ell=0}^{\infty} p_{\ell}^2 b_{\ell}^{\text{N}} b_{\ell}^{\text{T}} C_{\ell}^{\text{NT}} \sum_{m=-\ell}^{\ell} |(\psi_{\mathbf{a}, \mathbf{b}})_{\ell m}|^2$$

# Wavelet covariance estimator

- Suitability of wavelets for detecting cross-correlations
- Wavelet covariance

$$\hat{X}_{\psi}^{\text{NT}}(\mathbf{a}, \mathbf{b}, \gamma) = \frac{1}{N_{\alpha\beta}} \sum_{\alpha, \beta} \nu_{\alpha\beta} W_{\psi}^{\text{N}}(\mathbf{a}, \mathbf{b}, \alpha, \beta, \gamma) W_{\psi}^{\text{T}}(\mathbf{a}, \mathbf{b}, \alpha, \beta, \gamma)$$

- Average over orientations

$$\hat{X}_{\psi}^{\text{NT}}(\mathbf{a}, \mathbf{b}) = \frac{1}{N_{\gamma}} \sum_{\gamma} \hat{X}_{\psi}^{\text{NT}}(\mathbf{a}, \mathbf{b}, \gamma)$$

- Theoretical wavelet covariance

$$X_{\psi}^{\text{NT}}(\mathbf{a}, \mathbf{b}, \gamma) = \sum_{\ell=0}^{\infty} p_{\ell}^2 b_{\ell}^{\text{N}} b_{\ell}^{\text{T}} C_{\ell}^{\text{NT}} \sum_{m=-\ell}^{\ell} |(\psi_{\mathbf{a}, \mathbf{b}})_{\ell m}|^2$$

# Comparison of wavelets

- Compare predicted signal-to-noise ratio

$$\text{SNR}_\psi(a, b) = \frac{\langle \hat{X}_\psi^{\text{NT}}(a, b) \rangle}{\Delta \hat{X}_\psi^{\text{NT}}(a, b)}$$

where

$$[\Delta \hat{X}_\psi^{\text{NT}}(a, b)]^2 = \sum_{\ell=0}^{\infty} \frac{1}{2\ell+1} p_\ell^4 (b_\ell^{\text{N}})^2 (b_\ell^{\text{T}})^2 \left[ \sum_{m=-\ell}^{\ell} |(\psi_{a,b})_{\ell m}|^2 \right]^2 [(C_\ell^{\text{NT}})^2 + C_\ell^{\text{TT}} C_\ell^{\text{NN}}]$$

- Similar technique used to compare real, harmonic and wavelet space techniques for detection of cross-correlations  
→ wavelets optimal on certain scales (Vielva et al. 2006)

# Comparison of wavelets

- Compare predicted signal-to-noise ratio

$$\text{SNR}_\psi(a, b) = \frac{\langle \hat{X}_\psi^{\text{NT}}(a, b) \rangle}{\Delta \hat{X}_\psi^{\text{NT}}(a, b)}$$

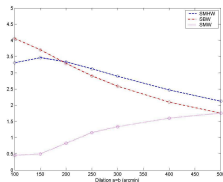
where

$$[\Delta \hat{X}_\psi^{\text{NT}}(a, b)]^2 = \sum_{\ell=0}^{\infty} \frac{1}{2\ell+1} p_\ell^4 (b_\ell^{\text{N}})^2 (b_\ell^{\text{T}})^2 \left[ \sum_{m=-\ell}^{\ell} |(\psi_{a,b})_{\ell m}|^2 \right]^2 [(C_\ell^{\text{NT}})^2 + C_\ell^{\text{TT}} C_\ell^{\text{NN}}]$$

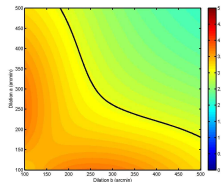
- Similar technique used to compare real, harmonic and wavelet space techniques for detection of cross-correlations  
→ wavelets optimal on certain scales (Vielva et al. 2006)

# Comparison of wavelets

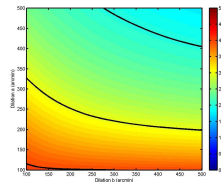
## SNR plots



(a) All wavelets



(b) SMHW



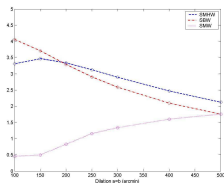
(c) SBW

**Figure:** Expected SNR of the wavelet covariance estimator of CMB and radio source maps

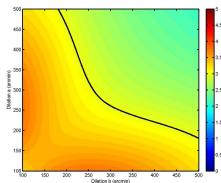
- Don't consider SMW further  
(actually considered; as expected not effective)

# Comparison of wavelets

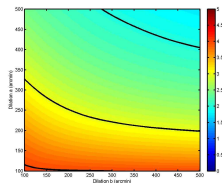
## SNR plots



(a) All wavelets



(b) SMHW



(c) SBW

**Figure:** Expected SNR of the wavelet covariance estimator of CMB and radio source maps

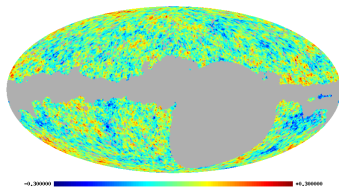
- Don't consider SMW further  
(actually considered; as expected not effective)

# Outline

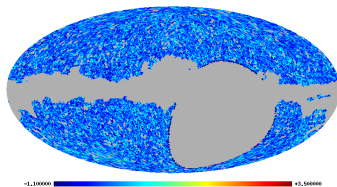
- 1 Integrated Sachs-Wolfe (ISW) effect
  - Physical origin
  - Detecting the effect
- 2 The continuous spherical wavelet transform (CSWT)
  - Dilations and mother wavelets on the sphere
  - Transform
- 3 Cross-correlation in wavelet space
  - Wavelet covariance estimator
  - Comparison of wavelets
- 4 **Analysis procedure**
- 5 Results
  - Detections
  - Dark energy constraints
- 6 Summary

# Analysis procedure

- Data



WMAP1



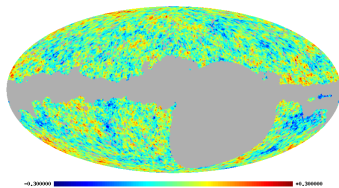
NVSS

- Analysis (scales; masks)
- Simulations
- Constraints on dark energy parameters

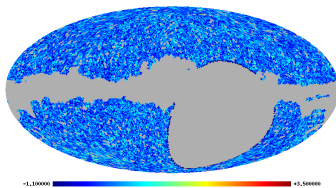


# Analysis procedure

- Data



WMAP1

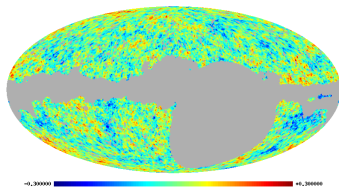


NVSS

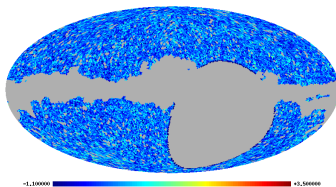
- Analysis (scales; masks)
- Simulations
- Constraints on dark energy parameters

# Analysis procedure

- Data



WMAP1

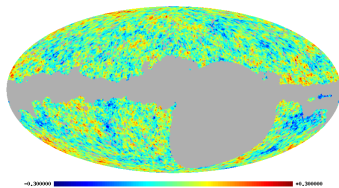


NVSS

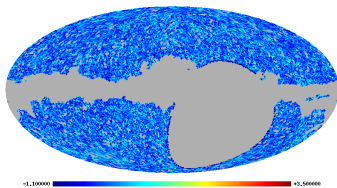
- Analysis (scales; masks)
- Simulations
- Constraints on dark energy parameters

# Analysis procedure

- Data



WMAP1



NVSS

- Analysis (scales; masks)
- Simulations
- Constraints on dark energy parameters

# Outline

- 1 Integrated Sachs-Wolfe (ISW) effect
  - Physical origin
  - Detecting the effect
- 2 The continuous spherical wavelet transform (CSWT)
  - Dilations and mother wavelets on the sphere
  - Transform
- 3 Cross-correlation in wavelet space
  - Wavelet covariance estimator
  - Comparison of wavelets
- 4 Analysis procedure
- 5 Results**
  - Detections
  - Dark energy constraints
- 6 Summary

# Scales and detections

- Scales

Scale	1	2	3	4	5	6	7
Dilation a	100'	150'	200'	250'	300'	400'	500'
Size on sky 1	282'	424'	565'	706'	847'	1130'	1410'
Size on sky 2	31.4'	47.1'	62.8'	78.5'	94.2'	126'	157'

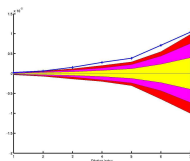
- Wavelet covariance plots

# Scales and detections

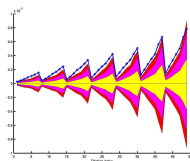
- Scales

Scale	1	2	3	4	5	6	7
Dilation a	100'	150'	200'	250'	300'	400'	500'
Size on sky 1	282'	424'	565'	706'	847'	1130'	1410'
Size on sky 2	31.4'	47.1'	62.8'	78.5'	94.2'	126'	157'

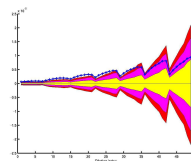
- Wavelet covariance plots



SMHW



SMHW



SBW

# Significance of detections

- Most significant detections
  - Wavelet covariance statistics appear Gaussian
    - $N_\sigma$  direct indication of significance of detections
    - symmetric SMHW:  $3.6\sigma$ ; elliptical SMHW:  $3.9\sigma$ ; SBW:  $3.9\sigma$
- $N_\sigma$  plots (2 and  $3\sigma$  contours)

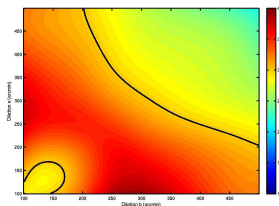
# Significance of detections

- Most significant detections
  - Wavelet covariance statistics appear Gaussian
    - $N_\sigma$  direct indication of significance of detections
  - symmetric SMHW:  $3.6\sigma$ ; elliptical SMHW:  $3.9\sigma$ ; SBW:  $3.9\sigma$
- $N_\sigma$  plots (2 and  $3\sigma$  contours)

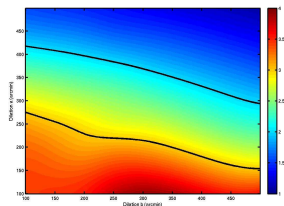


# Significance of detections

- Most significant detections
  - Wavelet covariance statistics appear Gaussian
    - $N_\sigma$  direct indication of significance of detections
  - symmetric SMHW:  $3.6\sigma$ ; elliptical SMHW:  $3.9\sigma$ ; SBW:  $3.9\sigma$
- $N_\sigma$  plots (2 and  $3\sigma$  contours)



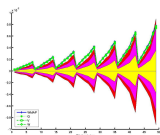
SMHW



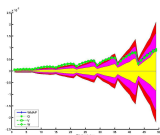
SBW

# Systematics and foregrounds

- Systematics: individual WMAP receiver maps  
→ systematics not likely source of detection
- Foregrounds: foreground dominated difference maps  
→ foregrounds not likely source of detection

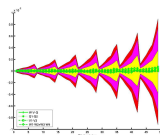


SMHW

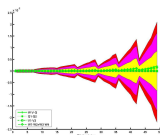


SBW

Individual receiver maps



SMHW



SBW

Difference maps

# Localised regions

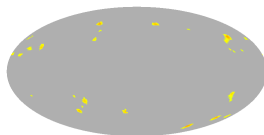
## Detection

- Wavelets inherently provide spatial localisation (in addition to scale localisation)
- Threshold wavelet coefficient product maps to localise most likely sources

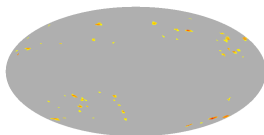
# Localised regions

## Detection

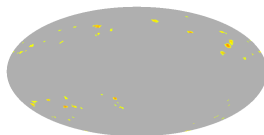
- Wavelets inherently provide spatial localisation (in addition to scale localisation)
- Threshold wavelet coefficient product maps to localise most likely sources



Symmetric SMHW



Elliptical SMHW

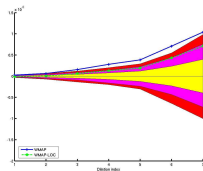


SBW

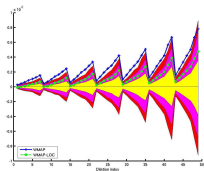
# Localised regions

## Removal

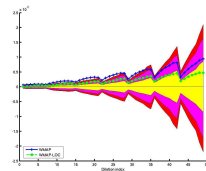
- Remove localised regions  $\rightarrow$  ISW detection remains  
(Agrees with findings of Boughn and Crittenden 2004)



Symmetric SMHW



Elliptical SMHW



SBW

- Examined localised regions in closer detail

# Dark energy constraints

- Compute theoretical wavelet covariance for range of models ( $w, \Omega_\Lambda$ )  
(assume concordance model for other parameters; bias  $b = 1.6$ )
- Compare theoretical predictions with observations

$$\chi^2(w, \Omega_\Lambda) = \Delta^T C^{-1} \Delta$$

where

$$\Delta = [\hat{X}_\psi^{\text{NT}}(a, b, \gamma) - X_\psi^{\text{NT}}(a, b, \gamma | w, \Omega_\Lambda)]$$

- Compute likelihood

$$\mathcal{L}(w, \Omega_\Lambda) \propto \exp[-\chi^2(w, \Omega_\Lambda)/2]$$

# Dark energy constraints

- Compute theoretical wavelet covariance for range of models ( $w, \Omega_\Lambda$ )  
(assume concordance model for other parameters; bias  $b = 1.6$ )
- Compare theoretical predictions with observations

$$\chi^2(w, \Omega_\Lambda) = \Delta^T \mathbf{C}^{-1} \Delta$$

where

$$\Delta = [\hat{X}_\psi^{\text{NT}}(a, b, \gamma) - X_\psi^{\text{NT}}(a, b, \gamma | w, \Omega_\Lambda)]$$

- Compute likelihood

$$\mathcal{L}(w, \Omega_\Lambda) \propto \exp[-\chi^2(w, \Omega_\Lambda)/2]$$

# Dark energy constraints

- Compute theoretical wavelet covariance for range of models ( $w, \Omega_\Lambda$ )  
(assume concordance model for other parameters; bias  $b = 1.6$ )
- Compare theoretical predictions with observations

$$\chi^2(w, \Omega_\Lambda) = \Delta^T \mathbf{C}^{-1} \Delta$$

where

$$\Delta = [\hat{X}_\psi^{\text{NT}}(a, b, \gamma) - X_\psi^{\text{NT}}(a, b, \gamma | w, \Omega_\Lambda)]$$

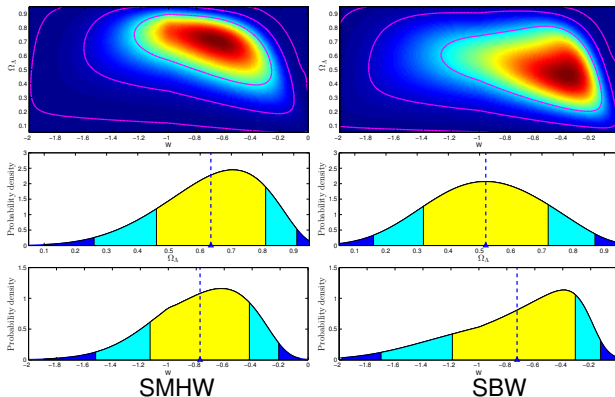
- Compute likelihood

$$\mathcal{L}(w, \Omega_\Lambda) \propto \exp[-\chi^2(w, \Omega_\Lambda)/2]$$



# Dark energy constraints

## Likelihood surfaces

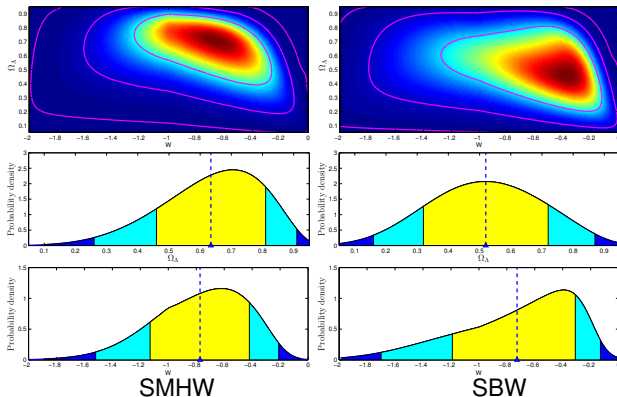


- Parameter estimates from mean of marginalised distributions

- $\Omega_\Lambda = 0.63^{+0.18}_{-0.17}$ ;  $w = -0.77^{+0.35}_{-0.36}$  using SMHW
- $\Omega_\Lambda = 0.52^{+0.20}_{-0.20}$ ;  $w = -0.73^{+0.42}_{-0.46}$  using SBW

# Dark energy constraints

## Likelihood surfaces

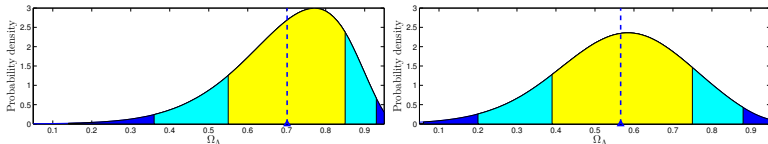


- Parameter estimates from mean of marginalised distributions

- $\Omega_\Lambda = 0.63^{+0.18}_{-0.17}$ ;  $w = -0.77^{+0.35}_{-0.36}$  using SMHW
- $\Omega_\Lambda = 0.52^{+0.20}_{-0.20}$ ;  $w = -0.73^{+0.42}_{-0.46}$  using SBW

# Dark energy constraints

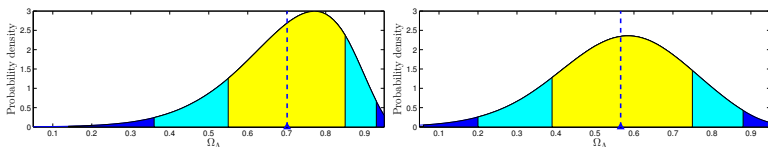
## Parameter estimates



- Also considered case  $w = -1$ 
  - $\Omega_\Lambda = 0.70^{+0.15}_{-0.15}$  using SMHW
  - $\Omega_\Lambda = 0.57^{+0.18}_{-0.18}$  using SBW
- Reject  $\Omega_\Lambda = 0$  at  $> 99\%$  significance
  - $\Omega_\Lambda > 0.1$  at 99.9% using SMHW
  - $\Omega_\Lambda > 0.1$  at 99.7% using SBW

# Dark energy constraints

## Parameter estimates



- Also considered case  $w = -1$ 
  - $\Omega_\Lambda = 0.70^{+0.15}_{-0.15}$  using SMHW
  - $\Omega_\Lambda = 0.57^{+0.18}_{-0.18}$  using SBW
- Reject  $\Omega_\Lambda = 0$  at  $> 99\%$  significance
  - $\Omega_\Lambda > 0.1$  at 99.9% using SMHW
  - $\Omega_\Lambda > 0.1$  at 99.7% using SBW

# Outline

- 1 Integrated Sachs-Wolfe (ISW) effect
  - Physical origin
  - Detecting the effect
- 2 The continuous spherical wavelet transform (CSWT)
  - Dilations and mother wavelets on the sphere
  - Transform
- 3 Cross-correlation in wavelet space
  - Wavelet covariance estimator
  - Comparison of wavelets
- 4 Analysis procedure
- 5 Results
  - Detections
  - Dark energy constraints
- 6 Summary

# Summary

- Used spherical wavelets to detect ISW effect
- Detection of ISW effect made at almost  $4\sigma$   
→ effectiveness of wavelets
- Foregrounds and systematics *not* likely source of detection
- Independent evidence of dark energy
- Consistent constraints on dark energy
  - Good consistency check with direct estimates from other approaches
  - Wavelets of similar performance for constraining dark energy as other ISW techniques